
Soft Tissue and Bone Infections

Rainer R. Schmitt and Georgios Christopoulos

Contents

1	General Aspects	263
1.1	Introduction	263
1.2	Routes of Infection	264
1.3	Imaging Techniques	264
2	Soft-Tissue Infections	266
2.1	Soft-Tissue Infections at the Fingers and Midcarpus	266
2.2	Suppurative Flexor Tenosynovitis	267
2.3	Tuberculosis of the Tendon Sheaths.....	268
2.4	Infections of the Deep Palmar Spaces.....	268
2.5	Gangrenous Infection	270
2.6	Pyomyositis and Necrotizing Fasciitis.....	270
3	Osteomyelitis	270
3.1	Time Course of Osteomyelitis	271
3.2	Etiology of Osteomyelitis	273
3.3	Differential Diagnosis	276
4	Infectious Arthritis	276
4.1	Bacterial Arthritis	277
4.2	Tuberculous Arthritis.....	277
5	Rare Infections of the Hand Skeleton	278
5.1	Syphilis	278
5.2	Gonococcal Arthritis	279
5.3	Leprosy (Hansen's Disease).....	279
5.4	Rare and Atypical Infections of Bacterial Origin....	280
5.5	Viral Infections	281
5.6	Fungal Infections	281
5.7	Parasitic Infections	282
6	Key Points	283
	References	283

R. R. Schmitt (✉) · G. Christopoulos
Institut für Diagnostische und Interventionelle Radiologie,
Herz- und Gefäß-Klinik GmbH, Salzburger Leite 1,
97616 Bad Neustadt an der Saale, Germany
e-mail: schmitt.radiologie@herzchirurgie.de

Abstract

Penetrating injuries and staphylococcal pathogens are the most frequent causes of infections at the hand, with the soft tissues involved in about 95%, and the bones and joints in 5%, only. In soft tissue infections, MRI is mostly necessary for depicting infections of the deep palmar spaces, whereas finger infections are prone to clinical examination. Typically, bone and joint infections are first visible in radiograms two weeks after clinical onset. MRI is powerful in early detection and in the assessment of spreading of both osteomyelitis and infectious arthritis, the adjacent soft tissues included. CT imaging is the modality of choice in the search of sequestra and cloaca when the superficial soft tissues and the skin are involved in chronic osteomyelitis. At the hands, rare infections are of tuberculous, syphilitic, leprous, viral, fungal, and parasitic origin.

1 General Aspects

1.1 Introduction

Infectious diseases of the hand affect the soft tissues, the bones, and the joints solely or in combination. In the past, the final diagnosis was made by clinical, laboratory findings, and radiographic survey views (Hausman and Lissner 1992). However, the approach toward dedicated diagnostic imaging has changed for several reasons in the last decade (Pineda et al. 2009; Santiago-Restrepo et al. 2003): First, imaging accuracy has significantly improved with the introduction of the high-resolution techniques of ultrasound, CT,



Fig. 1 Synopsis of the infectious pathways at the hand skeleton. **a** Direct pathways of infection with implantation or hematogenous spread of pathogens into the soft tissue (1), the joint (2), and the bone (3). Stars are used for symbolizing both the direct and hematogenous infection routes. **b** Indirect pathways comprising spreads of an infection from the soft tissues into the bone (4) or into the joint (5), and finally from the bone marrow into the adjacent joint and vice versa (6).

and MRI. Second, the advance of refined surgical and medical treatment options has increased the pretension according to detailed wrist and hand imaging. Third, the spectrum of hand infections has changed over the years with the expansion of the worldwide travel and the increasing number of surviving individuals suffering from immunodeficiency diseases.

Early diagnosis of hand infections is essential to prevent functional impairment or even destruction disease which usually remains secondary to delayed or insufficient treatment.

1.2 Routes of Infection

The soft tissues, bones, and joints of the hand can be contaminated by different routes (Fig. 1) (Tsai and Failla 1999; Resnick 1976):

- *Direct implantation of pathogens:* The infection arises directly after penetrating injuries with disruption of the overlying skin. This route is by far

c Marked thickening of the palmar digital bulb in the presence of a felon. The bony terminal phalanx is not involved. **d** In another case, infectious spread of a felon from the palmar soft tissues to the terminal phalanx is evident and has caused infectious bone destruction. **e** Subacute bacterial arthritis of the proximal interphalangeal joint immediately following a penetrating stab injury. There are deep erosions of the subchondral plates aside onset of sclerosing bone reaction

most frequent at the hands. In a similar pathway, pathogens can be incidentally inoculated during arthrography and arthroscopy, in open surgery as well as in transcutaneous insertion of pins.

- *Spread from a neighbored source of infection:* An infectious focus extends from one tissue layer to another, e.g. from the subcutis to the bones or joints, or from the bone marrow to an adjacent joint and the surrounding soft tissues, or from one to another communicating tendon sheath.
- *Hematogenous spread of infection:* Pathogens are inoculated via the blood circulation. Common sources of transient bacteremia are the respiratory, genitourinary, and gastrointestinal systems besides others and equivocal cases. This pathway is infrequent at the hands.

1.3 Imaging Techniques

Conventional radiograms (CR) complimented by fluoroscopic spot views in equivocal cases are

exposed to exclude or confirm inflammatory involvement of the hand skeleton. Eight to ten days usually pass before signs of osteomyelitis are visible. Early signs of acute osteomyelitis include subtle periosteal reaction and focal subperiosteal osteopenia (Capitanio and Kirkpatrick 1970). Osteolyses follow within the next weeks, and osteosclerosis appears in the chronic stage. Obliteration and swelling of the periarticular soft-tissue planes (“soft-tissue sign of arthritis”), periarticular osteopenia (“collateral sign of arthritis”) as well as articular destruction (“direct signs of arthritis”) appear in acute pyogenic arthritis and will progress in days to weeks. Soft-tissue calcifications are sometimes seen in tuberculosis of the tendon sheath.

Nuclear scintigraphy (NUC) with ^{99m}Tc phosphonates provides information about local hyperemia when using the three-phase technique (angiographic, blood pool, and delayed phases). For early detection of an infectious source, this technique is useful days and weeks before abnormalities become visible in radiograms (Gold et al. 1991). If scintigraphic results are unremarkable, an acute infection of the hand skeleton can be excluded. Soft-tissue infections lead to regional hyperemia with a diffuse nuclide uptake in the area involved and the contiguous bone skeleton. If soft-tissue infection directly spreads to the adjacent bones and joints, a marked nuclide uptake indicating hyperemic bone metabolism is mostly evident in three-phase scintigrams. However, positive scintigraphy does not allow differentiation between posttraumatic bone remodeling and infection, because an increased formation of fibrous bone, and therefore, an increased binding of ^{99m}Tc phosphonates is seen in both disease entities (Schauwecker 1989). This is also the case in chronic osteomyelitis. Differentiation can be tried with gallium scintigraphy which is sensitive to active bone disease (Pineda et al. 2009; Gold et al. 1991).

Scintigraphy with ^{99m}Tc -HMPAO-labeled leukocytes and ^{99m}Tc -nanocolloids as well as immunoscintigraphy with ^{99m}Tc -labeled monoclonal granulocytes or human unspecific immunoglobulin selectively demonstrates acute granulocyte-induced inflammations (Schauwecker 1989). There are some limitations: First, in the early months after an injury, leukocytic scintigraphy cannot differentiate between reparative remodeling and inflammatory processes. Second, in aseptic arthritis such as rheumatoid

arthritis and chronic infections such as tuberculous or leprous arthritis, uptake of labeled granulocytes can simulate findings of active osteomyelitis and pyogenic arthritis.

Ultrasonography (US) is the first-line imaging method when a fluid or abscess collection is assumed in the soft tissues and joint spaces (Kothari et al. 2001). For high-resolution US of the hands, probes of 10 MHz or more must be used. An important indication of US is the search for foreign bodies that are invisible in radiograms (Peterson et al. 2002). In the presence of osteomyelitis, involvement of the contiguous soft tissues can be screened with US.

Computed tomography (CT) is well suited to delineate the destructive bone processes in osteomyelitis, i.e. the sequestrum, the surrounding granulation tissue, and the involucrum. A sequestrum can be reliably detected in CT imaging by means of its dense eburnization and its location within the granulation tissue (Pineda et al. 2009; Santiago-Restrepo et al. 2003; Gold et al. 1991). Due to less sensitivity in comparison with MRI, CT is applied in the evaluation of soft-tissue inflammation in equivocal cases only for the search of foreign bodies and intraosseous or intraarticular air collections. Because osteomyelitis is often associated with soft-tissue infection, intravenous administration of a contrast agent is recommended for proper detection. The imaging features of an abscess are the peripheral enhancement and the semi-liquid abscess center (Kothari et al. 2001). Retrograde contrast-filling of a sinus tract (sinography) can be combined with CT scanning to depict the course of a sinus tract from the cutaneous orifice back to its medullary origin (Santiago-Restrepo et al. 2003). Finally, CT imaging—and also ultrasonography—is used for guiding percutaneous punctures of soft tissues, bones, and joints to obtain fluid for bacteriologic evaluation.

Magnetic resonance imaging (MRI) is very sensitive in detecting infections of the soft tissues, the bones, and joints and in depicting the extension of the inflammation (Pineda et al. 2009; Gold et al. 1991; Hopkins et al. 1995; Towers 1997; Morrison et al. 1993). The use of a dedicated surface coils or phased-array multi-channel coils is premise for MRI of the hand to obtain high-resolution images. In literature, the necessity of intravenous gadolinium is controversially discussed. According to the authors' experience, the administration of gadolinium is mandatory

for further characterizing infectious bone, joint, and soft-tissue edema. Differentiation between vascularized inflammatory tissue and central abscess colligation zone is facilitated with the use of gadolinium (Hopkins et al. 1995; Towers 1997; Morrison et al. 1993). However, it must be mentioned that MRI is inferior to CT imaging in detecting sequestra (Pineda et al. 2009; Gold et al. 1991). The T2-weighted fat-saturated FSE sequence (alternatively, the STIR-FSE sequence) and the T1-weighted fat-saturated SE sequence after gadolinium—both acquired in the transaxial plane—are most suitable to determine extra- and intraosseous inflammatory processes. The other imaging planes are crucial to determine the extent of the infection in the longitudinal direction.

2 Soft-Tissue Infections

In about 95% of all infections of the hand, exclusively the soft tissues are involved, namely the cutaneous, subcutaneous, fascial, tendinous, ligamentous, muscular, and synovial structures, whereas bones and/or joints are affected in only about 5% (Hausman and Lisser 1992; Tsai and Failla 1999). The heterogeneous spectrum comprises paronychia, felons, suppurative tenosynovitis, deep space infections, and gangrenous infections. The most common cause in etiology is a penetrating injury, while hematogenous spread is less frequent (Tsai and Failla 1999; Resnick 1976). Even the tiniest injury, such as a paronychial tear during nail care, is sufficient to inoculate pathogenic organisms. Individuals with a compromised immune system and/or sensory deficiency (e.g. patients suffering from diabetes mellitus or severe carpal tunnel syndrome) are predisposed to infections. In initial stages, infections mostly remain at the site of origin, since there are a number of anatomically defined compartments, like the subcutaneous space, the deep palmar spaces, the tendon sheaths, and the joint compartments. Clinical symptoms are local redness, hyperthermia, swelling, pain, and functional impairment.

Physical examination is usually sufficient for final diagnosis. However, when clinical uncertainty exists, diagnostic imaging can provide essential information for treatment decision, e.g. if an abscess in the deep spaces must be excluded or localized precisely (Beltran 1995). Furthermore, the pathogens can be

identified with ultrasound-guided aspiration to specifically initiate antibiotic medication.

2.1 Soft-Tissue Infections at the Fingers and Midcarpus

The following types of soft-tissue infection can be differentiated by location:

A *paronychia* is an acute infection of the space surrounding the eponychial fold, mostly caused by *Staphylococcus aureus*, less frequently by anaerobic or fungal pathogens (Jebson 1998a). Paronychial infections often begin after nail care and immediately spread around the eponychium to develop a purulent drainage. Lymphadenitis can be present. Chronic courses of paronychia caused by *Candida albicans* are seen in diabetic individuals.

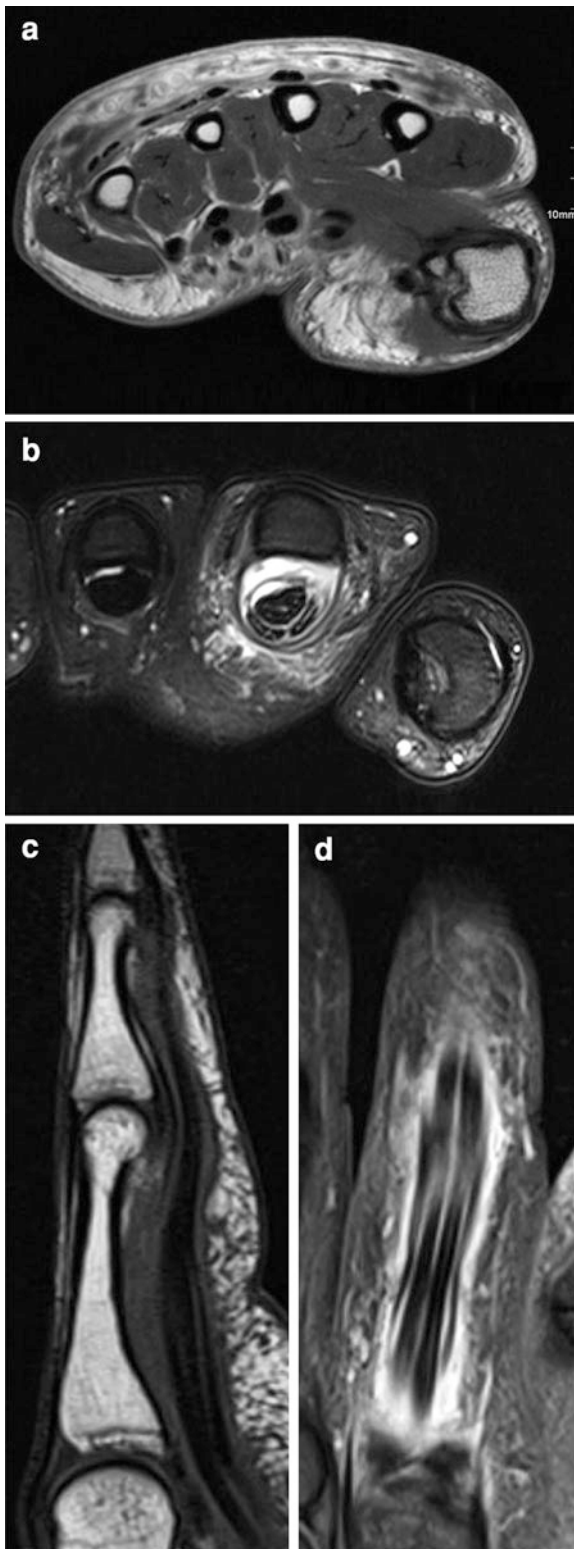
A *felon* is a closed space infection of the palmar digital bulb which can easily follow a skin lesion or a bagatelle injury (Jebson 1998a). The terminal phalanx is swollen, red, and painful.

A *collar button abscess* is a purulent infection of the interdigital subfascial web space (Jebson 1998b). Symptoms include painful swelling, redness, fluctuance, and tenderness of the web space with neighbored fingers being in an abducted posture.

A pyogenic *dumbbell infection* is located at the dorsoradial aspect and involves the thenar space, the first web and interosseous spaces, and the abductor pollicis muscle (Jebson 1998b). Mostly, the infection begins at the thenar space before extending into the peripheral and deep spaces.

Suppurative flexor tenosynovitis is a pyogenic infection of one or several flexor tendon sheaths which mostly is not only located at the digits but also in the midcarpal palm (Langer 2009).

In *radiograms*, swelling and obliteration of the tissue planes are characteristic. Bubbly gas inclusions are derived either from skin disruption or from gas-forming pathogens. Radiograms should always be ordered in the presence of phalangeal soft-tissue infection to confirm or exclude accompanying osteitis, osteomyelitis or even infective arthritis. Other than in paronychia, bone involvement is frequent in felons (Fig. 1c, d). When the infection has spread into the depth down to the osseous and/or articular surfaces, radiologic signs of osteitis include subtle periosteal thickening, indistinctly demarcated erosions,



◀ **Fig. 2** Contrast-enhanced MRI of suppurative soft infections. **a** Massive phlegmon (cellulitis) at the dorsum of the metacarpus. In the T1-weighted SE image after gadolinium, the subcutaneous layer appears thickened and presents with increased contrast enhancement. Areas of low signal intensity are included and are suspicious of initial abscess. **b–d** Suppurative flexor tenosynovitis of the index finger following an open cut injury. The flexor tendon sheath is semi-circumferentially thickened. After application of gadolinium, marked contrast enhancement of the tendon sheath is evident on the T1-weighted SE images with fat-saturation (**b** and **d**) when compared with the non-enhanced image (**c**). Areas of low signal intensity are not included, and therefore, abscess formation must not be assumed. Inflammation of the adjacent soft tissues is accompanying

and focal subperiosteal osteopenia (Capitanio and Kirkpatrick 1970). After progressing to osteomyelitis, sharp osteolyses appear. When subtle osteopenia of the subchondral articular bone plate becomes visible, concomitant arthritis of the metacarpophalangeal and interphalangeal joints must be assumed. Radiograms are also needed for the search of radiodense foreign bodies. Both US and MRI are useful tools for differentiating cellulitis from abscess formation in the soft tissues (Fig. 2a).

2.2 Supportive Flexor Tenosynovitis

Supportive tenosynovitis is caused by spread from a subcutaneous abscess or by a penetrating injury with inoculation of pathogens from which most common are *Staphylococcus aureus* and Streptococci (Langer 2009). The proximal interphalangeal joint and the middle phalanx are preferred sites of puncture wounds. Symptoms are summarized by the Kanavel's signs: Flexed posture and swelling of the affected digit, tenderness over the flexor sheath, and pain on passive extension of the digit. Lymphadenitis is usually present. Rarely, a V-shaped phlegmon involving two or more fingers can develop due to communicating tendon sheaths. More frequent is a phlegmon that migrates from the thumb proximally into the carpal tunnel thereby causing a hyperacute carpal tunnel syndrome.

Radiograms serve to exclude concomitant osteomyelitis and/or arthritis and to detect foreign bodies (Resnick 1976; Capitanio and Kirkpatrick 1970; Kothari et al. 2001). Osteopenia and cortical erosions at the neighbored bone may be evident. Infectious tenosynovitis can nicely be demonstrated with US

(Jeffrey et al. 1997). There is a thickened, moderately hyperechoic tendon sheath directly aside the hypo- to anechoic synovial fluid. An enclosed foreign body is detectable by means of its hyperechoic pattern and its distal acoustic shadow. Foreign bodies are usually found in the center of infections. The same diagnostic criteria apply for tenosynovitis in MRI (Fig. 2). The inflamed tendon sheath is thickened, hyperintense in T2-weighted sequences, and presents an intense, peripheral contrast enhancement in T1-weighted, fat-saturated sequences after gadolinium (Towers 1997; Beltran 1995). Intravenous gadolinium is helpful in differentiating encapsulated synovial fluid in tendon overuse from suppurative tenosynovitis, both presenting with a thickened synovium. The transaxial imaging plane is most important for detection, whereas both the coronal and sagittal planes enable precise assessment of the longitudinal extension of tenosynovitis. Often, secondary edema in the adjacent soft tissues and in the tendon itself (tendinitis) is accompanying.

2.3 Tuberculosis of the Tendon Sheaths

Musculoskeletal tuberculosis is currently beginning to rise again. *Mycobacterium marinum*, *avium* or *kansasii* are the pathogens (Hausman and Lissner 1992; Hoffman et al. 1996). Clinical symptoms are mild and inconclusive. Only a doughy, painless swelling along the flexor tendons can be present at clinical examination. Thus, the “great masquerader” of tuberculosis should always be taken into consideration when a palmar, indolent soft-tissue swelling of unknown origin fails to medical and surgical treatment.

Radiograms are usually normal in soft-tissue tuberculosis. Infrequently, foggy and indistinct spots of calcification can be found, but can be hidden by bony structures in standard views. CT is usually not indicated to search for these calcifications, but when performed for other reasons, peritendinous location of foggy calcifications is highly suggestive of tuberculosis. In the differential diagnosis, an acute inflammatory onset is suspicious for hydroxyapatite deposition disease, whereas a chronic, insidious course is characteristic of soft-tissue tuberculosis or sarcoidosis. In US, tuberculous tenosynovitis can be assessed by means of a synovial fluid and the thickened tendon sheaths, which is hyperechoic in comparison with non-tuberculous tenosynovitis. In MRI,

the tuberculous tendon sheaths appear distended and swollen and show a marked synovial contrast enhancement (Hoffman et al. 1996; Jaovisidha et al. 1996). These findings often contradict the minor patient’s symptoms and are therefore guiding for the final diagnosis (Fig. 3a). The differential diagnosis includes chronic tenosynovitis of other origin, e.g. tenosynovial sarcoidosis.

Aside the tendon sheaths, other soft-tissue compartment of the hands can be infected by atypical mycobacterial bacilli in individuals with impaired resistance (Hoyen et al. 1998). *Mycobacterium marinum* is seen in soft-tissue infections of fishermen and aquarium workers and *Mycobacterium terrae* in infections of gardeners (Fig. 3b).

2.4 Infections of the Deep Palmar Spaces

Superficial infections can continuously spread into the deep compartments of the palm, often with the primary infection already healed when the deep abscess becomes symptomatic. Pain and function impairment are almost always present. However, redness and swelling can be missed because superficial tissue is covering the affected spaces. In the depth, there are anatomically defined compartments (Fig. 4a) (Jebson 1998b): (1) the thenar space (built by the short muscles of the thumb), (2) the hypothenar space (built by the short muscles of the little finger), (3) the carpal tunnel (bordered by the palmar flexor retinaculum), (4) the Guyon’s canal (superficial and ulnar-sided to the carpal tunnel), (5) the Parona’s space (deep to the flexor tendons at the distal forearm), and (6) the metacarpal space (deep to the flexor tendons at the metacarpus).

Radiograms are only performed to exclude concomitant osteomyelitis. This is also possible with the use of skeletal scintigraphy (*NUC*). An abscess is classically visualized in US by means of an anechoic or hypoechoic center associated with distal acoustic shadowing, and a hyperechoic wall of granulation tissue (Jeffrey et al. 1997). Membranous septa are often seen within the abscess. However, there are some diagnostic limitations: While huge and focal abscesses are reliably detectable with US, small abscesses deep in the carpal tunnel remain difficult to visualize due to acoustic absorption phenomena of the superficially traversing flexor tendons. Furthermore, it is difficult to depict the entire extent of a



Fig. 3 Synopsis of the different sites of tuberculosis at the soft tissues and bones of the hand. **a** Tuberculous tenosynovitis in a female presenting with a doughy, painless swelling of her palm. In the contrast-enhanced T1-weighted SE scan with fat = saturation, there is a communicating tenosynovitis of the flexor pollicis longus and the flexor digitorum tendons at the levels of the Parona's space, the carpal tunnel, and the metacarpal space. **b** Tuberculous abscess in the subcutaneous layer of the thenar space (fat-saturated PD-weighted FSE image). Surprisingly, micro-bacterial evaluation revealed *Mycobacterium marinum* in this patient who was retrospectively identified as a hobby

angler. **c** Tuberculous dactylitis of the thumb in a 1-year-old infant. There is the characteristic spina ventosa of the first metacarpal bone with increased volume, central osteolysis, and thickened compact bone. **d** Tuberculous arthritis of the wrist in an advanced stage with destruction, collapse, and ankylosis of the carpus. The ongoing inflammatory process is indicated by cystic radiolucencies, indistinct joint contours, and soft-tissue swelling. Calcifications in the soft tissues are also seen. Figures **a**, **c**, and **d** with permission from Schmitt R, Lanz U. Diagnostic imaging of the hand and wrist. Thieme International. Stuttgart, New York 2008

multi-compartmental abscess formation and to differentiate it from a sympathetic effusion. Abscesses can also be detected and determined in size by using CT imaging, although its capability is inferior to that of MRI. In CT, the signs of an abscess are the semi-liquid center of about 30–50 HU and the peripheral, contrast-enhancing wall (Jaovisidha et al. 1996). Preferentially, MRI should be applied if an abscess of the deep palmar spaces is suspected (Fig. 4b, c). MRI

provides the most precise information for these purposes (Hopkins et al. 1995; Towers 1997; Beltran 1995). The semi-liquid center of an abscess is hyperintense in T2-weighted sequences and hypointense in T1-weighted sequences, in the latter with a strong peripheral enhancement seen after intravenous application of gadolinium. This pattern of contrast enhancement differentiates an abscess from a phlegmon as well as from a serous fluid collection.

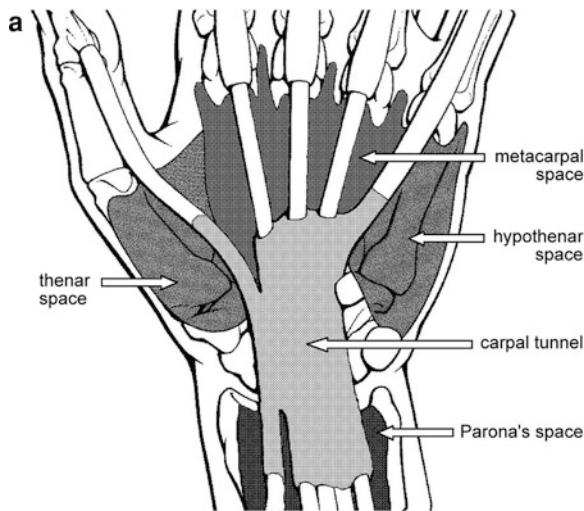
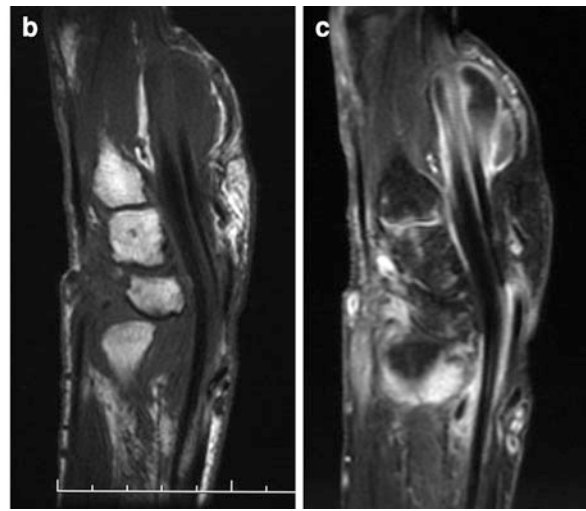


Fig. 4 Infections of the deep palmar spaces. **a** Schematic illustration of the deep palmar spaces (view into the palm). Indicated are the thenar and hypothenar spaces, the Parona's space (deep to the flexor tendons), the carpal tunnel, and the metacarpal space (deep to the flexor tendons). The Guyon's tunnel that is located ulnar-sided to the carpal tunnel is not depicted. **b–c** Deep palmar abscess extending over several deep



spaces. Sagittal T1-weighted SE images before (**b**) and after (**c**) application of gadolinium. The contrast-enhanced images comprehensively depict suppurative tenosynovitis of the flexor tendons in the Parona's space, the carpal tunnel, and the metacarpal space. Central areas of low signal intensity in the Parona's and metacarpal spaces are typical of an abscess formation

2.5 Gangrenous Infection

Gangrene is a rare anaerobic infection of the soft tissues caused by gas- and toxin-producing anaerobic pathogens (Hausman and Lisser 1992; Hoyer et al. 1998). The most common pathogen is *Clostridium perfringens*. The infection spreads in the subcutaneous space and within the compartments along the fasciae. Muscle ischemia and devitalized tissues may proceed and are considered as predisposing factors. The initial symptom can solely be local tenderness, followed by rapidly spreading inflammation. Cutaneous crepitation can be present, but does not confirm gangrenous infection. Life-threatening impairment of the general condition soon develops.

Survey radiographs characteristically show patchy gas inclusions in the soft tissues, especially in the subcutaneous and subfascial layers. Low-kilovoltage radiographs and CT imaging can be advantageous in equivocal cases.

2.6 Pyomyositis and Necrotizing Fasciitis

These infection types are extremely rare at the distal forearm and hand and are mentioned here for completeness only.

Pyomyositis is a muscle infection mostly caused by *Staphylococcus aureus* in immunodeficient patients (Gonzales 1998). The intra-muscular mass is characterized by an abscess formation in contrast-enhanced MRI (or CT imaging).

Necrotizing fasciitis is a serious, life-threatening infection of the superficial and deep fasciae in the absence of muscular and cutaneous infections (Gonzales 1998). Pathogens are *Streptococcus pyogenes* alone or in combination with *Staphylococcus aureus*. In imaging, the fasciae appear thickened and inflamed. Gas bubbles and fluid collections can be included.

3 Osteomyelitis

Osteomyelitis of the hand is usually the result of a soft-tissue infection caused by penetrating injuries with implantation of pathogens into the soft tissues and contiguous spread to the bone via the tendon sheaths, fasciae, and lymphatic vessels (Hausman and Lisser 1992; Tsai and Failla 1999; Resnick 1976; Barbieri and Freeland 1998). In open fractures, pathogens can be directly inoculated into the bone. These "secondary" types of osteomyelitis are

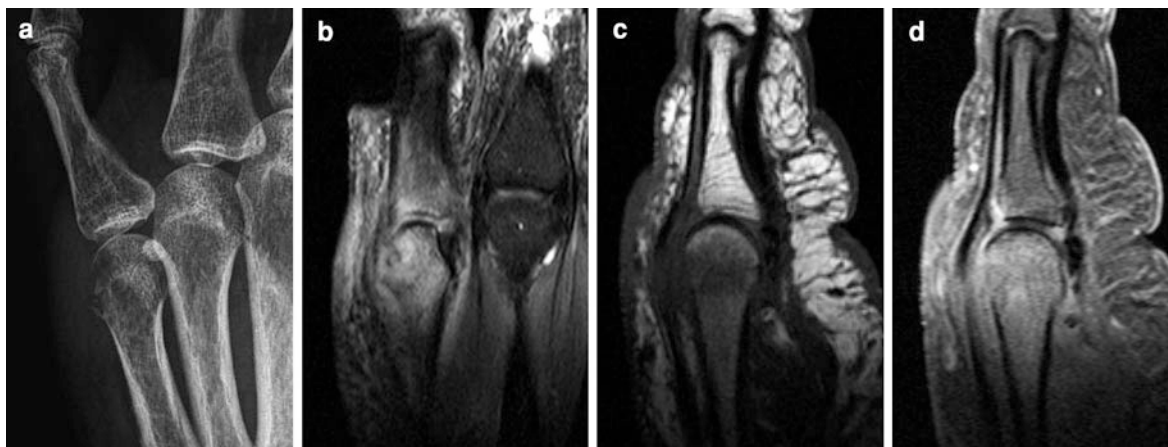


Fig. 5 Osteomyelitis and initial bacterial arthritis of the metacarpophalangeal joint of the little finger following a fist blow. **a** Obliteration of the soft-tissue planes and focal, subchondral demineralization at the dorso-ulnar segment of the fifth metacarpal head, depicted on a semi-pronated, oblique X-ray view. **b** Diffuse edema is present in the periarticular soft tissues as well as in the metacarpal head and the base of the

proximal phalanx (coronal, fat-saturated PD-weighted image). **c** and **d** Sagittal T1-weighted SE images before and after application of gadolinium without and with fat saturation show hyperenhancement of the dorsal soft tissues with the joint capsule and synovia included and in the inflamed bone marrow of the metacarpal head

frequent because the hands are predisposed to injuries in workaday life. On the contrary, the hematogenous spread of (“primary”) osteomyelitis is rare at the hand skeleton. The spectrum of pathogens includes *Staphylococcus aureus*, *Streptococcus pyogenes* and group B streptococci, and *Escherichia coli* (Tsai and Failla 1999; Barbieri and Freeland 1998; Reilly et al. 1997). Haemophilus influenza is a frequent pathogen in childhood, while fungal and tuberculous pathogens are more often seen in adulthood (Hoyen et al. 1998).

Osteomyelitis is defined as an infection of the bone marrow and the ossified bone substance itself (Pineda et al. 2009; Barbieri and Freeland 1998). Subcategories imply the osteitis (infection of the bone cortex) and the infectious periostitis (infection of the periosteal cloak). Further classification is based on the time course with differentiation of acute, subacute, and chronic osteomyelitis, all of them with fluent and non-definitive transitions (Pineda et al. 2009).

3.1 Time Course of Osteomyelitis

3.1.1 Acute Osteomyelitis

Acute osteomyelitis presents with acute redness, swelling, pain, and functional impairment of the hand area affected aside fever and general complaints (Tsai and

Failla 1999; Barbieri and Freeland 1998). Acute osteomyelitis leads to progressive bone destruction.

Radiograms provide the imaging basis of acute osteomyelitis (Pineda et al. 2009; Resnick 1976; Gold et al. 1991; Schauwecker 1989). However, one should keep in mind that radiologic findings lag behind the onset of the infection by about 8–10 days. The earliest signs include obliteration of the parossal soft tissue fat planes and a focal area of decreased bone density (Capitanio and Kirkpatrick 1970). In the next days, aggressive bone destruction follows in a permeative pattern. Radiolucent, poorly defined osteolyses appear at the infectious focus (Fig. 5a). Finally, the infection leads to endosteal scalloping and cortical disintegration, and subtle or marked periosteal lesions at the metaphyseal level. In the acute phase of osteomyelitis, MRI is the imaging method of choice for two reasons (Pineda et al. 2009; Santiago-Restrepo et al. 2003; Gold et al. 1991; Hopkins et al. 1995; Towers 1997; Morrison et al. 1993): First, inflammatory bone marrow edema is the earliest finding which can be appreciated with MRI as early as 3 days after the onset of infection. The edema and exudates within the medullary space produce ill-defined high signals on fat-suppressed T2-weighted or STIR images and a low signal on T1-weighted images (Figs. 5b, 6a). Second, contrast-enhanced T1-weighted images

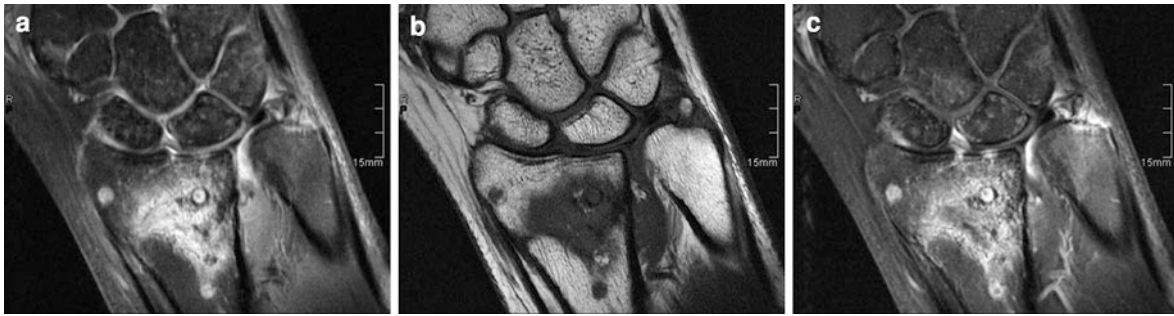


Fig. 6 Acute osteomyelitis of the distal end of the radius following 3 months after palmar plate osteosynthesis. After plate removal, X-ray views were completely unremarkable with regard to osteomyelitis. In MRI, a territorial zone of bone marrow edema (**a** and **b**) and peripheral contrast enhancement (**c**) is visible at the meta-epiphyseal section of the radius, and a

parossal abscess located in the soft tissues between the radius and ulna is also recognizable. PD-weighted FSE sequence with fat-saturation (**a**), non-enhanced T1-weighted SE sequence (**b**), and contrast-enhanced T1-weighted SE sequence with fat-suppression (**c**), all acquired in the coronal plane

acquired in 3 planes allow a comprehensive assessment of the osteomyelitic extent by better differentiation of hypervascularized areas from non-viable and edematous areas in the affected bone and the soft tissues (Figs. 5d, 6c).

Complete clinical information is required for the differential diagnosis of permeative (“moth-eaten”) bone lesions (Santiago-Restrepo et al. 2003; Resnick 1976; Capitanio and Kirkpatrick 1970). With this respect, healing of osteomyelitis can be correctly assessed only when judging both the clinical and imaging findings, because in the healing phase bone resorption is still continuing and simulating progressive osteomyelitis in radiograms, although the clinical symptoms are already improving (Erdman et al. 1991). The differential diagnosis includes malignant bone tumors, such as osteosarcoma, Ewing’s sarcoma, and bone lymphoma. In most cases, bone destruction in acute osteomyelitis is more rapid and extensive in comparison with the malignant tumors mentioned.

3.1.2 Subacute Osteomyelitis

Brodie’s Abscess

In staphylococcal osteomyelitis, an intra-osseous abscess can develop in individuals with immunologic deficiency, mainly in young boys. At the hand and forearm, there is a predilection for the distal ends of the radius and ulna. In *radiograms*, a round or elongated radiolucency with surrounding osteosclerosis, tortuous shape, and a connection to the growth plate is characteristic of a Brodie’s abscess (Pineda et al. 2009; Miller et al. 1979). In MRI, the so-called

“penumbra sign” is indicative. This sign describes a well-defined lesion which is composed of a central colliquation zone and a small peripheral zone of increased contrast enhancement surrounded by bone marrow edema in T1-weighted images (Grey et al. 1998). Mostly, Brodie’s abscesses are located in the metaphysis, less frequently in the epiphysis (Fig. 6). However, locations in the diaphysis and cortex have been described making differentiation to osteoid osteoma difficult even with the use of CT and MRI.

Plasma-Cell Osteomyelitis and Garré’s Sclerosing Osteomyelitis

These special forms of osteomyelitis are infrequently found at the hands (Reilly et al. 1997). They are characterized by the appearance of osteosclerosis and the tendency of a chronic course. A pathogen usually cannot be isolated, both entities are non-purulent. A pathogenetic association to chronic recurrent multifocal osteomyelitis has been assumed. The diagnosis of Garré’s osteomyelitis should be restricted to those cases of sclerosing osteomyelitis in which no sequestrum and granulation tissue can be found.

3.1.3 Chronic Osteomyelitis

The chronic stage is characterized by the development of sequestra, the formation of involucrum, and the deformation of the bone affected (Barbieri and Free-land 1998; Kaim et al. 2002). A *sequestrum* is a necrotic bone fragment which has developed from destruction of the cortical or cancellous bone (Pineda et al. 2009). Often, pathogens are harbored inside the sequestrum maintaining chronic osteomyelitis and

flare-up acute episodes. Surrounding *granulation tissue* separates the sequestrum from the viable bone. New bone formation is induced by the periostitis and is therefore located peripherally around the altered cortex and the necrotic tissue, the so-called *involucrum*. In many cases, infection-induced channels (so-called *sinus tracts*) are connecting the area of dead bone with the cutaneous surface composed of an osseous break (so-called *cloaca*) (Pineda et al. 2009).

In *radiograms*, a sequestrum has an increased radiodensity, sharp margins, and is located within the medullary bone (Pineda et al. 2009; Santiago-Restrepo et al. 2003; Gold et al. 1991; Kaim et al. 2002). The size varies from sub-millimeter to several millimeters. New bone formation, the involucrum, leads to contour irregularities, bone deformation, and increased radiodensity (Fig. 8). Differential diagnosis includes the osteoid osteoma which is frequently found at the hand, and the rare fibrous dysplasia. MRI is helping to assess the devitalized tissue in chronic osteomyelitis. A sequestrum is of low signal intensity in all sequences, whereas the surrounding granulation tissue is of high signal intensity in STIR or T2-weighted sequences, and of intermediate to low signal intensity on T1-weighted images. After application of gadolinium, the granulation tissue is enhancing, whereas the sequestrum remains low signal (Hopkins et al. 1995; Towers 1997; Morrison et al. 1993). The involucrum has low signal intensity on all pulse sequences and is separated from the cortical bone by a periosteal reaction zone which is of intermediate signal intensity on T2-weighted or STIR images (Pineda et al. 2009; Gold et al. 1991). The periosteal reaction zone is highly suspicious of containing infectious material, when presenting as a mass of high signal intensity on T2-weighted images. In this area of infection, a break traversing both the cortical bone and the involucrum is characteristic of a cloaca. Often, a sinus tract extends from the cloaca and appears with a tram track-like enhancement in the adjacent soft tissues before reaching the cutaneous surface with an orifice (Santiago-Restrepo et al. 2003). In chronic osteomyelitis, CT is particularly useful to identify a sequestrum and to differentiate between granulation tissue and an involucrum (Fig. 8c, d). Therefore, CT is essential for planning surgical therapy, and—most importantly—for detecting sequestra which must be excised (Pineda et al. 2009; Santiago-Restrepo et al. 2003; Gold et al. 1991).

Differentiation of active from inactive osteomyelitis is of high clinical importance, but challenging in diagnostic imaging (Erdman et al. 1991). Ongoing activity of infection must be assumed when the radiologic appearance has changed in follow-up studies, and when a sequestrum or a subperiosteal cloaca is still provable. A disadvantage of MRI is the inability to distinguish infectious from reactive inflammation (Pineda et al. 2009).

3.2 Etiology of Osteomyelitis

3.2.1 “Primary” (Hematogenous) Osteomyelitis

In septicemia, the respiratory, genitourinary, gastrointestinal systems, and the skin serve as infectious sources which however remains unknown in up to 50% of the cases (Hausman and Lisser 1992; Pineda et al. 2009; Barbieri and Freeland 1998). Infrequently, hematogenous spread of pathogens leads either to acute osteomyelitis of the distal sections of the radius and ulna (Gold et al. 1991; Reilly et al. 1997) or to acute pyogenic arthritis of the wrist (Murray 1998). Hematogenous osteomyelitis usually originates in the metaphysis, where bacterial implantation is facilitated by the slow blood flow in the venous sinusoids. Both bone marrow edema and accumulation of pus increases the bone pressure and promote further osteomyelitic extension which follows an age-dependent pattern (Resnick 1976): (a) In infants up to 1 year, only a few metaphyseal vessels penetrate the bone plate to reach the epiphysis and therefore being responsible for simultane osteomyelitis and purulent arthritis in infancy. However, the combined infection is difficult to detect due to the unossified epiphyses at this age. (b) In children and adolescents, the metaphyseal vessels turn sharply at the open growth plate without penetrating them. This unique pattern of vascularity explains the predilection of juvenile osteomyelitis to affect the dia-metaphysis only. (c) In adulthood, many metaphyseal vessels are connected to the epiphyseal vessels via the closed bone plate. This free vascular communication allows metaphyseal osteomyelitis to migrate to the epiphysis.

Radiograms show “moth-eaten” osteolyses and less often sequestra (Resnick 1976; Capitanio and Kirkpatrick 1970). Later in the course, periostitis and periosteal bone formation is more extended when compared

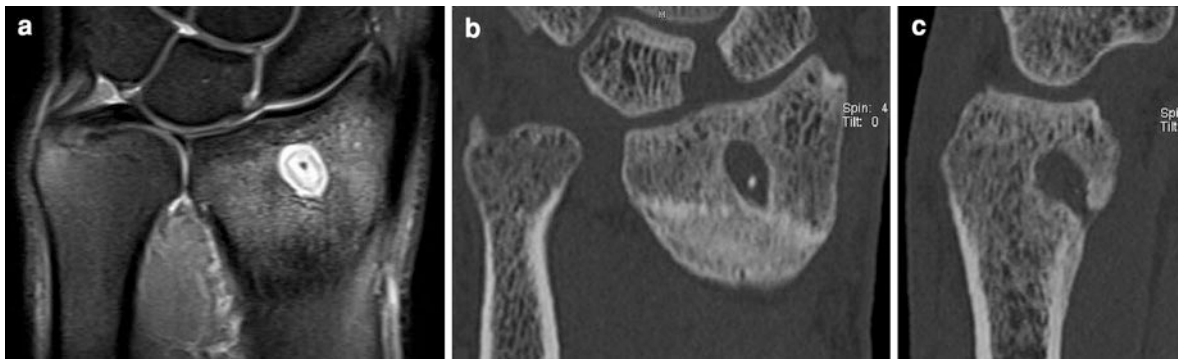


Fig. 7 Brodie's abscess in the distal end of the radius in a young man with no history of trauma or bone surgery. At the meta-epiphyseal junction, a sequestrum surrounded by an abscess and the so-called “double-line sign” are seen in a

coronal PD-weighted sequence with fat-saturation (a). Reformatted CT images in the coronal (b) and sagittal (c) planes confirm the sequestrum and prove the presence of a cloaca on the palmar site of the radius

to secondary osteomyelitis spread from soft-tissue infection. Chronic osteomyelitis is characterized in radiograms by bone remodeling with more or less intense osteosclerotic areas. Even the primary development of chronic sclerosing osteomyelitis is possible. MRI is the modality of choice for early diagnosis, therapy planning, and the follow-up (Hopkins et al. 1995; Towers 1997; Morrison et al. 1993). It provides all the information about the extension of osteomyelitis, particularly about soft-tissue complications. Osteomyelitic abscesses and osteonecrosis can be detected with fat-saturated T1-weighted sequences after intravenous administration of gadolinium. *Skeletal scintigraphy* is suitable to exclude or confirm the presence of osteomyelitis before lesions can be detected in plain radiograms, especially if MRI is not available (Pineda et al. 2009; Schauwecker 1989).

3.2.2 “Secondary” (Spread From Soft Tissues) Osteomyelitis

Secondary forms of osteomyelitis develop from the adjacent soft tissues. At the hand, secondary osteomyelitis is much more frequent in comparison with primary osteomyelitis (Hausman and Lisser 1992; Tsai and Failla 1999; Resnick 1976).

Osteomyelitis of the Fingers

Phalangeal manifestation is by far the most common form of osteomyelitis at the hands with the distal phalanx being most often affected. The inoculation of pathogens is caused by two different ways: First, the organisms reach directly the periosteum or bone via

the disrupted skin and the deep tissue layers. With this respect, even surgery can result in osteomyelitis, e.g. the pin tract infection (Tsai and Failla 1999). Second, there is initially a soft-tissue infection like a felon or suppurative flexor tenosynovitis after a puncture wound (Hausman and Lisser 1992; Beltran 1995; Jeffrey et al. 1997). These soft-tissue infections do not only extend longitudinally via the tendon sheaths and the fascial planes but also invade into the depth. The soft-tissue focus causes initial periostitis, then infectious invasion of the cortex, and finally osteomyelitis after invading the medullary bone via the cortical haversian and Volkmann's canals (Resnick 1976). Frequently, the formation of sequestra can result and maintain chronic fistulae.

In *radiograms*, positive findings cannot be expected in the first 10 days after an injury (Resnick 1976; Capitanio and Kirkpatrick 1970; Gold et al. 1991). As the result of the inward migrating infection from the soft tissues, discrete focal osteopenia and mild periostitis are the initial signs in osteomyelitis of the digits (Fig. 5a). Bone destruction with “moth-eaten” and permeative osteolyses subsequently follows. Finally, osteosclerotic transformation is typical of chronic osteomyelitis (Fig. 8). The radiologic examination should always include the search for foreign bodies which can cause and maintain infections of the fingers (Peterson et al. 2002). MRI is useful for depicting the infected soft tissues—particularly to prove or rule out an abscess (Fig. 6)—and for assessing the extension of osteomyelitis (Hopkins et al. 1995; Towers 1997; Morrison et al. 1993). However, the vast majority of paronychia and felons



Fig. 8 Two patients suffering from chronic osteomyelitis of the finger skeleton. **a** and **b** In the first patient, X-rays show increased bone density of the proximal phalanx due to marked periosteal reaction with initial development of an involucrum and a cloaca. The periosteum is elevated at the dorsum. **c** and **d** In the second patient, all signs of chronic osteomyelitis are

present in the index finger. In the metacarpal bone, several sequestra surrounded by granulation tissue, cloacae at the palmar and dorsal sites and an involucrum can be depicted in the transaxial (**c**) and sagittal (**d**) CT images. A *pin* has been introduced in the metacarpal base

do not involve the bone of the distal phalanx, and therefore, the role of MRI is mainly to exclude osteomyelitis. The use of CT is limited mainly for detecting sequestra (Figs. 7, 8) and intra-osseous abscesses (Kothari et al. 2001).

Bites

Bites at the hands are mostly caused by domestic animals, less frequent by humans, e.g. a fist blow to the mouth of the opponent (Gonzalez et al. 1993). Staphylococcal or streptococcal species are inoculated through the wound, particularly *Eikenella corrodens* in human bites, and *Pasteurella multocida* in cat bites (Resnick 1976). The rate of infectious complications such as soft-tissue infection, bacterial arthritis, and osteomyelitis is up to 50%. Symptoms are dominated by diffuse soft-tissue swelling, redness, impairment or loss of function and the local bite defect.

In *radiograms*, foreign bodies in the soft tissues must be excluded. In oblique views, subtle cortical lesions can sometimes be detected at the injury site after a deep bite down to the bone surface (Resnick 1976; Capitanio and Kirkpatrick 1970). Mostly, however, radiologic signs of osteomyelitis and/or bacterial arthritis appear first in about 8–10 days after the injury.

3.2.3 Special Forms of Osteomyelitis

Tuberculous Osteomyelitis

Skeletal tuberculosis that is a hematogenous infection caused by the *Mycobacterium tuberculosis* complex develops in the post-primary stage of tuberculosis. Pulmonary tuberculosis is evident in about half of the cases, but mostly inactive at the time of skeletal manifestation. Overall, the hands are involved only in

about 5% of musculoskeletal tuberculosis with two age groups (Hoyen et al. 1998; Benkeddache and Gottesman 1982; Hsu et al. 2004): Tuberculous osteomyelitis is more common in children under 5 years, while tuberculous arthritis is mostly manifested in adults. However, transition of tuberculous osteomyelitis to tuberculous arthritis has been observed, and also the reversed infection route. Other than in pyogenic infections, meta-epiphyseal spread of tuberculous osteomyelitis is possible in childhood. Clinical presentation at the hand skeleton is characterized by a chronic course and by a wide range of symptoms (Benkeddache and Gottesman 1982). It is not unusual that painless swelling, focal tenderness, and a draining sinus are noticed over months to years before the final diagnosis is found. One should consider that incidence of tuberculosis is currently increasing.

Radiologic signs of tuberculous osteomyelitis are heterogeneous. They include soft-tissue swelling, diffuse osteopenia, “moth-eaten” osteolyses, and marked bone expansion when periosteal bone formation has been induced (Benkeddache and Gottesman 1982). One metacarpal or phalangeal bone is affected in about 70% of tuberculous infections, two or several bones in the remaining cases. The affected bones appear thickened and with increased radiodensity. Both tuberculous bone thickening and soft-tissue swelling leads to a sausage-like deformity of the ray affected. The clinical condition is termed “tuberculous dactylitis”, and the radiographic appearance is the “spina ventosa” presenting with characteristic cyst-like bone expansion (Fig. 3c). Differential diagnosis of dactylitis also includes osteomyelitis of pyogenic, syphilitic, fungal, and leprosy origin as well as fibrous dysplasia, sarcoidosis, hyperparathyroidism, and sickle cell anemia. Sequestra are uncommon in skeletal tuberculosis. Osteosclerotic bone is seen at the thickened periosteum and at the borders of marginal erosions in case of concomitant tuberculous arthritis. In contrast-enhanced MRI, an intense, ring-shaped enhancement is observed at the small tubular bone(s) affected in tuberculous osteomyelitis (Hsu et al. 2004).

Chronic Recurrent Multifocal Osteomyelitis

Chronic recurrent multifocal osteomyelitis (CMRO) is a rare, aseptic condition of osteomyelitis seen in

children and adolescents and is characterized by a prolonged or fluctuating course. Aside psoriatic skin lesions, osteomyelitic lesions of unknown origin appear synchronously (Kothari et al. 2001). Causative organisms are usually not identified, and therefore, both immunologic phenomena and a genetic predisposition have been discussed in the pathogenesis. Probably, there is an association to the entities of plasma-cell osteomyelitis and Garre’s sclerosing osteomyelitis.

In *radiograms*, involved bones have findings typical of osteomyelitis and/or Brodie abscess with osteosclerotic lesions side by side with osteolytic destruction. The clavicles and the bones of the lower extremity are preferred locations. *Scintigraphy* is useful in identifying the multifocal involvement of CRMO (Kothari et al. 2001). Contrast-enhanced MRI is well suited for the follow-up.

3.3 Differential Diagnosis

Osteosarcoma and Ewing’s sarcoma are very rare at the hand skeleton. These malignant bone tumors must be taken into differential diagnostic consideration, when moth-eaten or permeative lesions are found in the metaphysis or diaphysis of the short tubular bones of the hand and when typical inflammatory signs are initially absent in osteomyelitis. Furthermore, advanced soft-tissue sarcomas can also lead to bone destruction and can simulate the radiographic pattern of osteomyelitis. However, soft-tissue sarcomas as well as their osseous spread are rare at the hands.

4 Infectious Arthritis

Infectious arthritis is an acute joint disease which is either caused by the articular implantation of a pathogen (“primary infectious arthritis”) or is triggered as an immunologic answer (“reactive post-infectious arthritis”) following a nasopharyngeal, respiratory, urogenital or intestinal infection, e.g. acute rheumatic fever following streptococcal tonsillitis (Resnick 1976; Murray 1998). The discussion of whether infectious arthritis manifests in parallel with or complementary to an immunologically induced bacterial arthritis is ongoing.

Staphylococci are the most common pathogens in about 70% of all bacterial joint infections (Hausman and Lisser 1992; Murray 1998; Graif et al. 1999). Some group preferences are evident: Streptococci and *Haemophilus influenzae* are frequently seen in children, *Neisseria gonorrhoeae* in young women, and gram-negative rods in patients with immune deficiency. Tuberculous, viral or parasitic pathogens can be isolated less commonly (Hoyen et al. 1998). Chlamydia, *Borrelia burgdorferi* (Lyme disease), *Mycobacterium leprae*, *Schistosoma haematobium* as well as hepatitis B and rubella viruses have been identified aside others in the synovial fluid recently. Risk factors of acquiring septic arthritis include diabetes mellitus, liver cirrhosis, alcohol or drug abuse, malignancy, and the advanced age.

4.1 Bacterial Arthritis

Three different pathways (Tsai and Failla 1999; Resnick 1976) are possible in pyogenic joint inflammation (Figs. 1a, b): First, bacterial arthritis is caused by spread of soft-tissue infection or by osteomyelitic transmission from a neighbored bone. This pathway is mostly seen at the finger joints. Second, pathogens can be directly inoculated via a penetrating injury as occurring in cuts, stabs and bites, and artificially during a diagnostic or surgical procedure at the joint. All joints of the hand can be involved in this pathway, but the metacarpophalangeal and proximal interphalangeal regions are clearly preferred (Resnick 1976). Third, bacterial arthritis arises from hematogenous seeding of pathogens in patients suffering from severe sepsis or severe immunologic deficiency. The carpal joints are mostly affected by hematogenous arthritis (Murray 1998).

The distribution pattern of pyogenic arthritis is usually monoarticular (Resnick 1976). The symptoms comprise low-grade fever, chills, and the focal signs of infection (swelling, redness, heat, arthralgia, tenderness). The classical disease course begins at the synovial membrane which becomes thickened and edematous, thereby producing synovial fluid and pus. The inflamed, pannus-like synovium initially induces cartilage destruction, and then leads to deep erosions at the subchondral bone plate. Depending on the violence of the pathogen, the infected joint is progressively destroyed.

In *radiograms*, signs of pyogenic arthritis follow a time-dependent pattern (Resnick 1976; Murray 1998; Gonzalez et al. 1993). Initially, obliteration of the periarticular soft-tissue planes (so-called “soft-tissue sign”) and a widened joint space caused by an infectious joint effusion are seen. Intra-articular gas formation is occasionally recognizable in gram-negative bacterial arthritis. Hyperemia-induced osteopenia is evident in about 8–10 days later (Fig. 9a), at first in the subchondral bone plate, then covering the entire epiphyseal area (so-called “collateral sign”). Synovial inflammation (Figs. 9b, e) leads subsequently to focal bone erosions at the bare areas and soon involves the entire articular space with poorly defined margins and progressive destruction of the joint (so-called “direct sign of arthritis”). The joint space narrows progressively with advanced destruction of the articular cartilage. Coarse erosions and destructive joint collapse are characteristic radiographic findings in bacterial arthritis (Fig. 9d–f). Finally, fibrous or bony ankylosis can develop at the end of the healing process. Another complication is the development of secondary osteoarthritis.

Most cases of infectious arthritis at the hand can be assessed clinically. At the wrist, the differential diagnosis includes rheumatoid arthritis, which however presents with a typical articular distribution pattern at the hands, and tuberculous arthritis, which progresses more slowly compared to bacterial arthritis (Graif et al. 1999). However, differential diagnosis can be challenging when other joint diseases like the calcium pyrophosphate dehydrate (CPPD) deposition disease, gout arthropathy or rheumatoid arthritis precede the joint infection (Murray 1998). In this situation, indium- or technetium-labeled leukocyte bone scans may be useful for differentiation (Pineda et al. 2009; Schauwecker 1989).

4.2 Tuberculous Arthritis

Tuberculosis osteomyelitis is commonly seen in children, while tuberculous arthritis is mostly affecting adults suffering from other underlying disorders (Hoyen et al. 1998; Benkeddache and Gottesman 1982; Hsu et al. 2004). The pathways of tuberculous arthritis comprise either primary joint infection or initial osteomyelitis followed by secondary spread to the joint(s). Typically, the latter is characterized by a



Fig. 9 Hematogenous arthritis of the wrist in a 52-year-old woman. Probably, the staphylococcal dissemination originated from an acute maxillary sinusitis. The image collection includes the initial imaging findings **a–c** 15 days after onset of the symptoms, and a follow-up examination **d–f** 4 weeks later for monitoring the antibiotic therapy response. **a–c** Initial imaging findings: diffuse osteopenia of the wrist, no erosions detectable (**a**). In the PD-weighted FSE sequence with

fat-saturation (**b**) and in the non-enhanced T1-weighted SE image (**c**), diffuse bone marrow edema, carpal joint effusions, and synovitis are evident. **d–f** Follow-up imaging findings: multi-locular erosions have developed at the wrist bones and the distal forearm. While deep erosions can already be seen in the dorso-palmar X-ray view (**d**), the finest erosions are only detectable in the contrast-enhanced T1-weighted SE sequence with fat-saturation (**e**) and in high-resolution CT (**f**)

less destructive course. The stages from articular swelling to final joint destruction are passed through slowly over a period of months to years.

In *radiograms*, signs of tuberculous arthritis are first seen in about 2–4 months after the onset of symptoms (Hoyen et al. 1998; Benkeddache and Gottesman 1982). The radial side of the wrist and midcarpus are mainly affected. The radiographic features are best summarized by the Phemister’s triad consisting of periarticular osteopenia, peripheral erosions, and mild joint space narrowing (Fig. 3d): The initial signs are soft-tissue swelling and periarticular osteopenia. The joint space is preserved over a long time, but is finally narrowing as the tuberculous synovitis progresses. Fine erosions at the subchondral bone plate lead to delineation of the articular contours. In contrast, marginal punched-out defects and central defects caused by granulomatous proliferation are characteristic of the cystic form of carpal tuberculosis which presents with a “nibbling of cheese” pattern. Extensive bone destruction and fibrous or

bony ankylosis can develop if antituberculous medication is delayed or insufficient. Calcifications are observed in concomitant soft-tissue abscesses and during healing. In early stage of tuberculous arthritis, the differential diagnoses include non-infectious arthropathy such as rheumatoid arthritis, skeletal sarcoidosis in case of cystic tuberculosis, and more unlikely the pyogenic arthritis.

5 Rare Infections of the Hand Skeleton

5.1 Syphilis

The spirochete *Treponema pallidum* is the pathogen of congenital syphilis as well as in acquired syphilis (Hoyen et al. 1998; Sachdev and Bery 1982). Symptoms of the survived congenital infection include saber shins, a saddle nose, palate perforation, and the



Fig. 10 Venereal infections of the hand. **a** Characteristic syphilitic dactylitis. In this child, dactylitis was limited to the metacarpal bone of the left thumb. The affected bone is increased in volume and radiodensity due to massive periosteal hyperostosis. Courtesy of Dr. A.M. Davies, Birmingham, UK. **b** Very rare case of an acquired gonococcal arthritis of the wrist in a 63-year-old woman. Marked osteopenia of the carpal, distal forearm, and the proximal metacarpal bones is evident. The heights of the radiocarpal and midcarpal cartilage are decreased, although there is a joint effusion with displaced soft-tissue planes. Pre-existing osteoarthritis of the trapezio-metacarpal joint

Hutchinson's triad (barrel-like teeth, keratitis, and nerve deafness). Three stages are discernable in the acquired disease: Focal skin ulceration develops at the site of infection (primary syphilis), followed by generalized skin eruption several weeks later (secondary syphilis). After healing, there is a prolonged syphilitic dissemination in almost all organ systems with the patients mostly being symptom-free. Many years later, about half of the patients develop cutaneous, cardiovascular, neurologic, and/or musculoskeletal symptoms due to granulomatous ("gummatous") lesions (tertiary syphilis). The hand skeleton is rarely involved.

Initially, the *radiographs* of newborns suffering from congenital syphilis reveal erosive irregularities at the epi-metaphyseal junctions induced by osteochondritis (Sachdev and Bery 1982). After these findings have disappeared, inflammatory enchondral and periosteal hyperostosis is causative of dense and thickened

tubular bones. Bilateral and symmetric involvement of the metacarpals or phalanges is characteristic of syphilitic dactylitis in childhood. The radiographic appearance resembles that of osteoidosteoma and tuberculous dactylitis (Fig. 10a). In tertiary syphilis, both the pathogenesis (osteochondritis, periostitis, and osteomyelitis) as well as the radiologic appearance is similar to that of tuberculosis, however, with the joints being less severely involved. The main finding is periosteal proliferation leading to significant enlargement of the tubular bones.

5.2 Gonococcal Arthritis

Gonococcal arthritis develops about 2 weeks after the venereal infection with *Neisseria gonorrhoeae*. Polyarticular symptoms are observed in gonococcal sepsis only. Thus, gonococcal infection should be considered in sexually active patients presenting with migratory polyarthralgias. Mostly, however, there is a monoarticular infection with the carpal joints being predominantly affected among other joints (Hoyen et al. 1998) (Fig. 10b). If no gonococci can be proved in the joint fluid, differential diagnosis should include reactive arthritis and the postgonococcal Reiter's syndrome.

5.3 Leprosy (Hansen's Disease)

In Africa, South America and Asia, leprosy is a chronic infection caused by *Mycobacterium leprae*. The clinical presentation is determined by an incubation period over months and combinations of neural, osseous, and dermal leprosy (Hoyen et al. 1998). Lymphadenopathy is seen in most cases. Involvement of peripheral nerves is characteristic, particularly with implantation of pathogens in Schwann's cells of the ulnar and peroneal nerves. Subsequently, progressive denervation with sensory and motor impairment leads to repetitive traumatic lesions and extensive superinfections. Leprous arthritis is either of hematogenous origin or spread from the leprosy bone marrow and the soft tissues. The joint infection is located at the carpal, metacarpophalangeal, and proximal interphalangeal joints. Finally, reactive arthritis can follow



Fig. 11 Rare bacterial, fungal, and parasitic infections at the hand. **a** Leprosy. There are acro-osteolyses at the terminal phalanges leading to the “candystick” deformity of the middle and ring fingers. Additionally, sclerosing osteomyelitis of the middle phalanx of the middle finger is visible. Courtesy of Dr. A.M. Davies, Birmingham, UK. **b** Mutilation stage of meningococcal infection in an infant with osteomyelitic destruction of the distal radial section and of the entire wrist. All fingers have been amputated before because of severe septic embolism.

Courtesy of Dr. A.M. Davies, Birmingham, UK. **c** Mycetoma of the hand in a child presenting with multi-locular soft-tissue masses and advanced osteopenia. Manifestation of mycetoma at the hand is very rare. Courtesy of Dr. A.M. Davies, Birmingham, UK. **d** Filariasis with detection of a calcified worm remnant in the soft tissue of metacarpus. This was an incidental finding in a woman suffering from known filariasis of her breasts. Courtesy of Dr. M. Langen, Würzburg/Germany

leprosy in a typically symmetric pattern and is associated with erythema nodosum.

Two different groups of leprosy abnormalities are visible in *radiograms* (Enna et al. 1971): First, specific granulomatous lesions directly induced by the pathogens are found at the metacarpal and phalangeal bones in less than 10% of musculoskeletal leprosy (osteitis leprosa multiplex cystica). Initially, soft-tissue swelling is evident followed by periostitis as the infection extends to the bones. Signs of leprosy osteomyelitis are focal osteopenia, enlarged nutrient channels, and finally advanced bone destruction. Second, unspecific neuropathic lesions account for the great majority of leprosy. Progressive bone destruction is the result of neuropathic articular malfunction, repetitive injuries, and additional superinfections. Neuropathic leprosy is associated with significant bone resorption and acro-osteolyses leading to the characteristic “candystick appearance” of the metacarpals and phalanges with the index finger predominantly affected (Fig. 11a). However, this radiographic appearance is also seen in Charcot’s osteoarthropathy as found in syringomyelia, syphilis, and diabetes mellitus. Due to limited access to advanced imaging techniques in the non-developed

countries, US and MRI are applied only in rare cases of neural leprosy for depicting the enlarged or compressed nerves (Martinoli et al. 2000). Finally, neural calcifications have been reported.

5.4 Rare and Atypical Infections of Bacterial Origin

These infections comprise a heterogeneous group with the hand skeleton being rarely involved (Hausman and Lissner 1992; Hoyer et al. 1998). The radiographic appearance is unspecific in most diseases. Occasionally, clinical or imaging findings can guide for final diagnosis, like the “doigt en lorgnette” aspect (shortened phalanges due to infectious bone resorption) in yaws (Jones 1972), or the late, but fulminant ball-and-socket destruction of the digits secondary to septic emboli in meningococemia (Patriquin et al. 1981) (Fig. 11b). Some infections do not affect the hand skeleton although the site of inoculation has been there, as seen in rickettsial-induced cat-scratch disease which is characterized by chronic lymphadenopathy proximally to the elbows. Essential information is summarized in Table 1.

Table 1 Rare and atypical infections of bacterial origin at the musculoskeletal system

Type of infection	Pathogen	Occurrence	Imaging findings
Yaws	<i>Treponema pertenue</i>	Africa South America South Pacific Islands West Indies	Similar to those of syphilis in secondary and tertiary yaws Phalanges thickened (“dactylitis”) or shortened (“doigt en lorgnette”) Distal phalanges spared
Meningococemia	<i>Neisseria meningitidis</i>	Ubiquitous	Fulminant in childhood late after meningococcal sepsis Ball-and-socket deformities of the fingers as the result of septic emboli
Lyme disease	<i>Borrelia burgdorferi</i> transmitted by the <i>Ixodes ricinus</i> tick	Ubiquitous Northeastern United States preferred	Joint effusions only No radiographic findings in the presence of intermittent and migrating arthralgia Chronic oligoarthritis very rarely
Brucellosis	<i>Brucella abortus</i> , <i>melitensis</i> or <i>suis</i>	Midwestern United States Saudi Arabia South America Southern Europe	Septic arthritis and osteomyelitis No specific manifestations on imaging Like “atypical” tuberculosis
Actinomycosis	<i>Actinomycis israelii</i>	Ubiquitous	Most frequent at mandible, spine and lung Hand very rarely affected Combination of osteolysis, sclerosis, and abscess

5.5 Viral Infections

Synovial infections have been observed in hepatitis B, rubella (measles), mumps, variola (smallpox), parvo-B19-infection, in vaccinia and others. The carpal, metacarpophalangeal, and proximal interphalangeal joints can be involved. Episodic, symmetric polyarthritis is observed which usually heals out. However, in adolescents growth disturbance can be associated. Carpal involvement can result in carpal tunnel syndrome.

Infections with *rubella* viruses can occur before birth (intrauterine rubella), or after birth (postnatal rubella), the latter induced either by contagious infection or by active immunization. The carpal and phalangeal joints are affected mostly by migratory symptoms, and only in rare cases erosive arthropathy resembling on juvenile chronic arthritis develops.

Variola (smallpox) is frequently manifested at the elbow joints, whereas the hands are typically spared. In the acute infection phase, radiographic signs are similar to those of purulent osteomyelitis or arthritis. The articular spread of variola tends to become chronic.

Patients suffering from the *human immunodeficiency virus (HIV)* infection do not provide a specific

infection pattern at the hands (Eustace et al. 1996). However, these individuals are often affected by opportunistic bacterial infections (septic osteomyelitis and/or arthritis, and pyomyositis), by seronegative spondylarthropathic diseases, and by the development of Kaposi’s sarcoma.

5.6 Fungal Infections

Fungal infections of the deep body layers and the musculoskeletal system are rare in comparison with their cutaneous manifestation (Amadio 1998). Almost always, individuals suffering from immunosuppression, malignant or chronic renal diseases are affected. Notably, candidiasis of the joints and bones is extremely rare, although *Candida* organisms reside on the human mucosal membranes. Fungal infections can be transmitted by traumatic inoculation of pathogens from the cutis into the depth or by hematogenous dissemination. Histoplasmosis, mycetoma (Fig. 11c), sporotrichosis, and coccidioidomycosis are tropical diseases which can induce polyostotic bone infections. None of the fungal diseases present with a

Table 2 Fungal infections at the musculoskeletal system

Type of infection	Pathogen	Occurrence	Imaging findings
Candidiasis (Moniliasis)	<i>Candida albicans</i>	Immunosuppression, antibiotic therapy, or diabetes mellitus common	Oral candidiasis, and disseminated abscesses In systemic candidiasis, osteomyelitis and arthritis extremely rare at the hand skeleton
Aspergillosis	<i>Aspergillus fumigatus</i>	Immunosuppression common	Mostly lung and chest wall affected Musculoskeletal system and hands rarely involved Localized bone destruction and soft-tissue mass
Coccidioidomycosis	<i>Coccidioides immitis</i>	United States Mexico South America	Lung and visceral dissemination Protuberances preferred in skeletal manifestation Well-defined osteolyses
Sporotrichosis	<i>Sporothrix schenckii</i>	Ubiquitous Immunosuppressed individuals preferred	Primary infection of the skin and lymph nodes Carpal and phalangeal joints often involved Marginal erosions and osteomyelitis
Histoplasmosis	<i>Histoplasma capsulatum</i> <i>Histoplasma dubosii</i>	United States Africa	Visceral and bone involvement common Cystic bone lesions at the wrist and hand skeleton
Mycetoma (Maduromycosis)	Mixed infection with <i>Actinomyces</i> , <i>Nocardia</i> , and <i>Streptomyces</i> pathogens	India Tropical climates Africa	Madura foot most common Chronic granulomatous infection of the subcutis and underlying bones Hand very rarely affected
Blastomycosis	<i>Blastomyces dermatitidis</i>	North America Central America South America	Lung, lymph nodes, and skin affected Skeleton involved in 50% of cases, the carpus included Unspecific bone destruction (erosions, osteomyelitis, osteoclerotic margins)
Cryptococcosis (Torulosis)	<i>Cryptococcus neoformans</i>	Ubiquitous	Predilection for the CNS Osteolytic foci at the axial skeleton and long bones, hand very rarely affected

specific radiographic appearance at the hand skeleton. The various symptoms range from self-limiting arthralgia over acute polyarthritis to mutilating joint destruction (Amadio 1998). The radiologic appearance is cystic or honey-combed or even erosive (Comstock and Wolson 1975). As a rule, fungal arthritis has a slow course when compared to acute pyogenic arthritis. As in other bone and joint infections, MRI provides detailed information about the extent of bone and soft-tissue involvement. Table 2 summarizes possible fungal infectious disease of the musculoskeletal system.

5.7 Parasitic Infections

Parasitic infections are extremely rare at the hands. Late in the natural disease course, dead parasites can cause bizarre calcifications in the soft tissues (Samuel 1950) (Fig. 11d). The form of these calcified remnants is either cystic (echinococcosis), spotty (cysticercosis) or linear and curled (filariasis, *Loa loa*, Guinea worm disease). When such atypical calcifications are detected and equivocal in origin, one should consider the presence of one of these rare parasitic infections.

6 Key Points

- Approximately 95% of all hand infections are located within the soft tissues, with only 5% involving bone or joint.
- The majority of superficial soft-tissue infections can be managed clinically without the need of imaging. However, radiographs, CT or MRI is required in two clinical settings: First, if spread of infection from the soft tissues to the adjacent bones or joints is suspected. Second, if a deep palmar abscess is suspected.
- In acute osteomyelitis, radiographic signs typically lag behind the onset of the infection by 8–10 days. In the majority of cases, initial findings are very subtle, before marked and poorly defined bone destruction appears.
- MRI is the most powerful imaging tool in detecting and comprehensively staging soft tissue and bone infections. Intravenous gadolinium is recommended for better differentiating abscesses from diffuse infections and the surrounding edema.
- CT imaging is best suited in chronic osteomyelitis for depicting the osseous structures, particularly for detecting sequestra that should be surgically removed to reduce the risk of reactivation of the osteomyelitis.
- Tuberculosis of the flexor tendon sheaths, the bones or the joints of the hands should be considered with slowly progressive infections associated with painless swelling and/or a draining sinus.
- Full clinical information is required for correct interpretation of the destructive bone and joint changes. Identification of the causative pathogen is mandatory to indicate the appropriate antibiotic therapy. Imaging-guided aspiration can be useful for this purpose.

References

- Amadio PC (1998) Fungal infections of the hand. *Hand Clin* 14:605–612
- Barbieri RA, Freeland AE (1998) Osteomyelitis of the hand. *Hand Clin* 14:589–603
- Beltran J (1995) MR imaging of soft tissue infection. *MRI Clin North Am* 3:743–751
- Benkeddache Y, Gottesman H (1982) Skeletal tuberculosis of the wrist and hand: a study of 27 cases. *J Hand Surg* 7:593–600
- Capitanio MA, Kirkpatrick JA (1970) Early roentgen observations in acute osteomyelitis. *Am J Roentgenol* 108:488–496
- Comstock C, Wolson AM (1975) Roentgenology of sporotrichosis. *Am J Roentgenol* 125:651–655
- Enna CD, Jacobson RB, Rausch RO (1971) Bone changes in leprosy: a correlation of clinical and radiologic features. *Radiology* 100:295–299
- Erdman WA, Tamburro F, Jayson HT, Weatherall PT, Ferry KB, Peshock RM (1991) Osteomyelitis: characteristics and pitfalls of diagnosis with MR imaging. *Radiology* 180:533–539
- Eustace SJ, Lan HH, Katz J et al (1996) HIV arthritis. *Radiol Clin North Am* 34:450–453
- Gold RH, Hawkins RA, Katz RD (1991) Bacterial osteomyelitis: findings on plain radiographs, CT, MR, and scintigraphy. *Am J Roentgenol* 157:365–370
- Gonzales MH (1998) Necrotizing fasciitis and gangrene of the upper extremity. *Hand Clin* 14:635–645
- Gonzalez MH, Papierski P, Hall RF (1993) Osteomyelitis of the hand after a human bite. *J Hand Surg* 18A:520–522
- Graif M, Schweitzer ME, Deely D et al (1999) The septic versus nonseptic inflamed joint. MR characteristics. *Skeletal Radiol* 28:616–620
- Grey AC, Davies AM, Mangham DC et al (1998) The “penumbra sign” on T1-weighted MR imaging in subacute osteomyelitis: frequency, cause and significance. *Clin Radiol* 53:587–592
- Hausman MR, Lisser SP (1992) Hand infections. *Orthop Clin North Am* 23:171–185
- Hoffman KL, Bergman AG, Hoffman DK et al (1996) Tuberculous tenosynovitis of the flexor tendons of the wrist: MR imaging with pathologic correlation. *Skeletal Radiol* 25:186–188
- Hopkins KL, Li KCP, Bergman G (1995) Gadolinium-DTPA-enhanced magnetic resonance imaging of musculoskeletal infectious processes. *Skeletal Radiol* 24:325–330
- Hoyen HA, Lacey SH, Graham TJ (1998) Atypical hand infections. *Hand Clin* 14:613–634
- Hsu CY, Lu HC, Shih TT (2004) Tuberculous infection of the wrist: MRI features. *Am J Roentgenol* 183:623–628
- Jaovisidha S, Chen C, Ryu KN et al (1996) Tuberculous tenosynovitis and bursitis: imaging findings in 21 cases. *Radiology* 201:507–513
- Jebson PJL (1998a) Infections of the fingertip. *Hand Clin* 14:547–555
- Jebson PJL (1998b) Deep subfascial space infections. *Hand Clin* 14:557–566
- Jeffrey RB Jr, Laing FC, Schechter WP et al (1997) Acute suppurative tenosynovitis of the hand: diagnosis with US. *Radiology* 162:471–472
- Jones WP (1972) Doigt en lorgnette and concentric bone atrophy associated with healed yaws osteitis. *J Bone Joint Surg Br* 54:341–345
- Kaim AH, Gross T, von Schulthess GK (2002) Imaging of chronic posttraumatic osteomyelitis. *Eur Radiol* 12:1193–1202

- Kothari NA, Pelchovitz DJ, Meyer JS (2001) Imaging of musculoskeletal infections. *Radiol Clin North Am* 39:653–671
- Langer MF (2009) Pyogenic flexor tendon sheath infection: a comprehensive review. *Handchir Mikrocir Plast Chir* 41:256–270
- Martinoli C, Derchi LE, Bertolotto M et al (2000) US and MR imaging of peripheral nerves in leprosy. *Skeletal Radiol* 29:142–150
- Miller WB, Murphy WA, Gilula LA (1979) Brodie abscess: reappraisal. *Radiology* 132:15–23
- Morrison WB, Schweitzer ME, Bock GW et al (1993) Diagnosis of osteomyelitis. Utility of fat-suppressed contrast-enhanced MR imaging. *Radiology* 189:251–257
- Murray PM (1998) Septic arthritis of the hand and wrist. *Hand Clin* 14:579–587
- Patriquin HB, Trias A, Jecquier S et al (1981) Late sequelae of infantile meningococemia in growing bones of children. *Radiology* 141:77–82
- Peterson JJ, Bancroft LW, Kransdorf MJ (2002) Wooden foreign bodies: imaging appearance. *Am J Roentgenol* 178:557–562
- Pineda C, Espinosa R, Pena A (2009) Radiographic imaging in osteomyelitis: the role of plain radiography, computed tomography, ultrasonography, magnetic resonance imaging, and scintigraphy. *Semin Plast Surg* 23:80–89
- Reilly KE, Linz JC, Stern PJ, Giza E, Wyrick JD (1997) Osteomyelitis of the tubular bones of the hand. *J Hand Surg Am* 22:539–644
- Resnick D (1976) Osteomyelitis and septic arthritis complicating hand injuries and infections: pathogenesis of roentgenographic abnormalities. *J Can Assoc Radiol* 27:21–28
- Sachdev M, Bery K, Chawla S (1982) Osseous manifestations in congenital syphilis: a study of 55 cases. *Clin Radiol* 33:319–323
- Samuel E (1950) Roentgenology of parasitic calcification. *Am J Roentgenol* 63:512–522
- Santiago-Restrepo C, Giménez CR, McCarthy K (2003) Imaging of osteomyelitis and musculoskeletal soft tissue infections: current concepts. *Rheum Dis Clin North Am* 29:89–109
- Schauwecker DS (1989) Osteomyelitis: diagnosis with In-111-labeled leukocytes. *Radiology* 171:141–146
- Towers JD (1997) The use of intravenous contrast in MRI of extremity infection. *Semin Ultrasound CT MR* 18:269–275
- Tsai E, Failla JM (1999) Hand infections in the trauma patient. *Hand Clin* 15:373–386